REPORT DOCUMENTATION PAGE

AFRL-SR-AR-TR-09-0214

PLEASE DO NOT RETURN YOUR FORM TO THE ABOVE ADDRESS.

1. REPORT DATE *(DD-MM-YYYY)*	2. REPORT TYPE	3. DATES COVERED (From – To)
	Final Technical Report	1 JAN 2004 – 30 JUNE 2007

4. TITLE AND SUBTITLE
AN EXPERIMENTAL STUDY OF THE RECEPTIVITY OF A COMPRESSIBLE LAMINAR BOUNDARY LAYER

5a. CONTRACT NUMBER

5b. GRANT NUMBER
FA9550-04-1-0026

5c. PROGRAM ELEMENT NUMBER

6. AUTHOR(S)
PROFESSOR GARRY L. BROWN

5d. PROJECT NUMBER

5e. TASK NUMBER

5f. WORK UNIT NUMBER

7. PERFORMING ORGANIZATION NAME(S) AND ADDRESS(ES)
P.O. BOX CN 5263
PRINCETON, NJ 08544-5263

8. PERFORMING ORGANIZATION REPORT NUMBER

9. SPONSORING/MONITORING AGENCY NAME(S) AND ADDRESS(ES)
USAF/AFRL
AFOSR
875 North Randolph Street
Arlington VA 22203

10. SPONSOR/MONITOR'S ACRONYM(S)
AFOSR

11. SPONSORING/MONITORING AGENCY REPORT NUMBER
N/A

12. DISTRIBUTION AVAILABILITY STATEMENT

Distribution Statement A: Approved for public release. Distribution is unlimited.

13. SUPPLEMENTARY NOTES

14. ABSTRACT

It remains true that in numerous compressible flows the prediction of transition and ist sensitivity to various disturbances has a major impact on system performance. It is also probably true that the least well understood aspect of the onset of transition in a supersonic boundary layer is the receptivity of the boundary layer to free stream acoustic disturbances and free stream turbulence.

15. SUBJECT TERMS

16. SECURITY CLASSIFICATION OF:			17. LIMITATION OF ABSTRACT	18. NUMBER OF PAGES	19a. NAME OF RESPONSIBLE PERSON
a. REPORT	b. ABSTRACT	c. THIS PAGE			19b. TELEPONE NUMBER (*Include area code*)
Unclassified	Unclassified	Unclassified	Unclassified	18	(703)

AN EXPERIMENTAL STUDY OF THE RECEPTIVITY OF A COMPRESSIBLE LAMINAR BOUNDARY LAYER

03NA144

AFOSR Contract Number FA9550-04-1-0026

Final Report for the period January 1, 2004 through June 30, 2007

Prepared for:

Dr John Schmisseur
Air Force Office of Scientific Research
801 N. Randolph St.
Arlington, VA 22203-1977

Principal Investigator:

Professor Garry L. Brown
Princeton University
D-222 E-Quadrangle, Olden St.
Princeton, NJ 08544
glb@princeton.edu
609-258-6083

October, 2008

1. Abstract

It remains true that in numerous compressible flows the prediction of transition and its (unknown) sensitivity to various disturbances has a major impact on system performance. It is also probably true that the least well understood aspect of the onset of transition in a supersonic boundary layer is the receptivity of the boundary layer to free stream acoustic disturbances and free stream turbulence (vorticity and entropy fluctuations). Very well defined experiments are required to advance fundamental understanding and to validate CFD simulations. Advances in CFD, validated with high quality experiments, will enable new understanding and the development of new tools for the prediction of compressible transition. This work has led to the development of a pure tone acoustic disturbance in a Mach 3 free-stream which drives a forced response in the boundary layer. The run time for each experiment is approximately a minute. Techniques have been developed (for this short run time) which have enabled the rejection of the 'naturally occurring' boundary layer response to other free stream disturbances. As a result this background signal level on the hotwires, apart from the specific driving signal, has been reduced from approximately .25-3mV (after band pass filtering in the 8-10 KHZ band) to 4-48 microvolt. This has enabled highly accurate measurements to be made of the phase and amplitude of the forced response and has led also to an accurate correction for temperature effects. An x-t diagram has been created from the experimental results. The diagram and the corresponding detailed collapse of the wave packet measurements show an oblique acoustic wave in the free stream traveling at 1003m/s and amplifying boundary layer wave-packets which travel at 392m/sec and 424m/sec. Measurements have now been made at the leading edge and they show that the receptivity to the leading freestream wave packet is practically zero and that the instability waves are generated by the following reflected free stream acoustic disturbances which have a different spanwise wavelength from the leading packet. We postulate that the greater receptivity to these free stream disturbances is the result of a better matching in spanwise wavelength. These results were made definitive by further measurements and they were followed by a direct attempt to drive a u-a disturbance from the nozzle sidewall. A simulation of the propagation of the wave front was achieved (reported at the Program Manager's meeting in August 2007) which became the basis of the experimental design. Experimental results for this case showed that the technique was remarkably successful.

2. Introduction

2.1 Earlier results and the foundation for the Research

In the first stage of our work, emphasis was placed on characterizing the free stream disturbances in the wind-tunnel in the "naturally occurring" case, measuring the development of linear instability and measuring some principal features of transition. These measurements have been analyzed, written up and published [1]. The experiments showed that with laminar tunnel wall boundary layers the remaining corner disturbances were the primary source of free-stream fluctuations at low tunnel stagnation pressures, and that these fluctuations were acoustic. The non-dimensional propagation speed of these free-stream disturbances (with respect to free-stream velocity) was found to be ~ 0.64, a value which yields stream-wise wavelengths which are remarkably close to the wavelengths of the corresponding first mode instability waves. With assumptions for the

receptivity, Federov, (Appendix in [1]) has made predictions from stability theory of the amplitude and growth rate which agree well with the measurements at frequencies within the unstable range, in this "naturally occurring" case. By contrast, at lower frequencies for which stability theory predicts a decaying disturbance, the measurements show a growing disturbance in the boundary layer (and also in the free stream). The receptivity to the free-stream mass flux fluctuation (density-velocity product) was found experimentally to give a relatively large ratio of 10 for the amplitude of the peak boundary layer fluctuation to the free-stream fluctuation at R~ 700, and at approximately the most unstable frequency [1].

This work provided a foundation for subsequent work which has focused on the receptivity of the boundary layer and in particular the receptivity to an imposed single frequency acoustic free-stream disturbance. This allows detailed measurements to be made of the initial forced response in the boundary layer and of the evolution of this response at frequencies of unstable eigen modes as well as at lower frequencies where eigen modes are damped.
Receptivity experiments for incompressible flows have focused on the isolation of the T-S wave from the background disturbances. Examples can be found in a recent review by Saric et al (2002). The major difficulty in the study of supersonic receptivity comes from the "naturally occurring" free-stream disturbances which are responsible for the "naturally occurring" linear instability waves in the boundary layer (Graziosi & Brown 2002). When an external acoustic forcing is applied, the forced boundary layer response is contaminated by this background T-S wave at the same frequency. Also, in the compressible case if the forcing is continuous, it is difficult to isolate the forced instability wave from a direct response of the boundary layer (Stokes wave) since it is expected that the principal receptivity is not confined to the leading edge region.

2.2 The concept for the Research

This work has focused on the receptivity of a Mach 3 boundary layer and in particular the receptivity to an imposed single frequency acoustic free-stream disturbance. This allows detailed measurements to be made of the initial forced response in the boundary layer and of the evolution of this response at frequencies of unstable eigen modes.
Driving a free stream acoustic field in the test section of a supersonic tunnel using an acoustic source in the settling chamber has been attempted by a number of investigators in the past but abandoned because a measurable disturbance, at frequencies of interest, was not obtained. For the conditions of the present experiment, however, the laminar boundary layer is relatively thick so that the frequencies of interest (4kHz – 15kHz) are relatively low and well within the range of a loudspeaker. In addition to the fact that in the "naturally occurring" case the free-stream disturbances in our previous experiments were acoustic (with laminar wall boundary layers, as in "quiet" tunnels), there are many compelling experimental advantages in using a pure tone disturbance and in this research we have continued to improve our techniques to obtain acoustic forcing with a pure tone and a well defined wave vector.

The Mach 3, low turbulence, tunnel used in these experiments is operated at a low stagnation pressure of approximately 3.6 psia. It is the same facility as described in

reference (1). At this pressure the tunnel wall boundary layers are laminar (with the exception of residual disturbances measured in the nozzle corner) and the free stream disturbance level is < 0.11%. The experiments in reference (1) showed that this residual free stream disturbance was acoustic and that it led to an amplifying response in the boundary layer.

The more recent work began with the recognition that high frequency oblique acoustic waves should be readily transmitted through the throat and that the acoustic wave vector would be refracted by the increase in velocity. To reduce reflected power, and account for the refraction of the wave packet, a 66^0 wave duct aimed towards the throat, has been used (Figure 1.). Continuous acoustic forcing at 8.9 kHz with the loudspeaker located as in Fig.(1) was then readily measured in the spectrum of the free stream hotwire fluctuations, downstream at Mach 2.98 above the plate.

Forcing with a wave packet has important advantages over continuous forcing because it is possible, in principle, to reduce reflections and multi-path effects, and to measure propagation speeds of a specific wave packet with ideally a single wave vector. In principle, the locally forced response in the boundary layer to this free stream disturbance can then be separated from an upstream boundary layer response which subsequently amplifies and propagates downstream with a different wave velocity. With wave packet forcing, however, the overall signal level is much less than in the continuous case and a particular effort is required to extract the wave packet from the naturally occurring disturbances. With an increasing understanding of the experimental results, numerous refinements have been made to the experimental details for both the creation of the wave packet and the signal processing to extract the wave packet in the free stream and the boundary layer. The key to a very much higher noise rejection ratio is to exploit the precise wave propagation time from the loud speaker to the hotwire in the free stream. The corresponding noise rejection then results from ensemble averaging signals in which the speaker driving voltage is used as the reference signal and as a trigger to the data acquisition system; this ensures that all signal records are aligned with respect to the origin of the wave packet (to better than 1 microsecond). Thus the hotwire signals were first filtered with 8 to 10 kHz band pass filters and then the data records were ensemble averaged to extract the wave packet and reject the noise. Figure 2. shows the locations (not to scale) where hotwire measurements were obtained in the free-stream and in the boundary layer

3. Results

Figure 3 shows the driving voltage to the loud speaker for a packet of eight waves and the corresponding, ensemble-averaged, delayed response (due to the distance from the speaker) measured by two hotwires above the plate, one in the free-stream and the other in the boundary layer. Figure 4 shows a measurement in the boundary layer with a fixed delay between wave packets of 30 ms and with 2600 samples and the much improved result with a variable shorter time (>17 ms) between samples and with 4400 samples. This variable time between packets overcame the problem of acoustic reflections arriving from the previous pulse which then corrupt the data from this next pulse. This technique increased the noise rejection substantially and led to the low remaining noise levels, at

different locations (i.e. 4-48 micovolt), as shown in Table I. Figure 5a shows the ensemble averaged signals of two hot wires in the free stream and separated in x and y. The amplitude distribution suggests a leading wave packet followed by three weaker packets. These three later packets are the result of different path lengths (and wavc vectors) once the wave packet leaves the duct from the loud speaker and travels to the test section. (Experiments in the no-flow case showed that only eight to ten waves formed the packet which leaves the acoustic duct and the weak waves from duct reflections arrive at much later times). Figure 6 illustrates how the reflections arise although it is much simplified and takes no account of the initial refraction due to the acceleration of thc flow. (These results were simulated by following acoustic wave crests from the duct to the test section and the results were presented as a movie at the Program Manager's meeting in July 2007.) Figure 5b shows the very high level of repeatability of the data even in the boundary layer at the largest downstream location and from runs on different days (the shift in arrival time accounts for temperature differences)). Figure 7 shows the first wave-packet in figure 5 (a) on an expanded scale; from a direct correlation between the two hotwire signals and the driving signal we find the time shift between the two signals, which leads to a measurement of the wave speed of this packet based on the distance between the wires. Figure 8 shows the second wave packet in figure 5a on an expanded scale and it shows that it is traveling at a different (higher) specd corresponding to a different wave vector direction (larger angle with respect to the free stream and a longer path length (later time) roughly in accord with expectations from figure 6). Figure 9 shows the first wave-packet signals for a free-stream probe and a boundary layer probe at the same x location and these comparisons at three different x locations. These results show that the leading wave packet in the boundary layer is a direct rcsponse to the free stream forcing (i.e. there is no measurable delay between the first wave packet in the boundary layer and in the free stream) and the signal ratio at all x locations is close to 2.5. We recognize that all velocities in this compressible flow scale with the stagnation speed of sound (assuming a perfect gas). Thus, from the measured mean stagnation temperature over a run, we can correct the arrival time of the first wave packet when it is measured at different locations both in the boundary layer and in the free stream and on different days. Figure 10 shows this data. It is immediately clear that the source of the scatter is the precise speed of propagation from the speaker to the probe. This speed however scales exactly with the square root of the stagnation temperature (perfect gas) so we can use the arrival time to essentially measure the temperature and find a corrected temperature (not exactly the more approximate experimental measurement) such that all first wave-packets would arrive at this location at the same time if the temperature were the reference temperature. This requires temperature corrections of only fractions of a degree up to 2 degrees which are within the experimental error of the temperature measurements made at that time. When corrected in this way Figure 11 shows an x-t diagram plotted from all of the measurements of the delay times for the arrival of the first wave packet at different x locations in both the boundary layer and the free-stream. This becomes a powerful tool in determining the velocities of the subsequent wave packets. Figure 12 shows the corresponding collapse of all the first wave packets measured in thc free stream and also shows that the subsequent packets in the free stream are not traveling at the same speed as this first packet. Figure 13 shows the corresponding collapse of the first wave packets in the boundary layer and it too shows that the subsequent packets in

the boundary layer do not travel at the same speed and indeed grow in amplitude and become much larger than the corresponding signal in the free-stream (figure 12). Figure 14 shows a complete x-t diagram for the boundary layer measurements based on the correction to a reference temperature. The amplitude as a function of time of the signal at each x location has been included in this figure and the "characteristics" for the wave packets are shown. The middle of the three characteristics for each of the three identified packets has been drawn from the average speed of the packet and it is found to connect accurately zero crossings. (This supports the calculation of the average speed). Figure 15 shows these results (without the middle characteristic) and the corresponding characteristics obtained from the free-stream measurements where the free stream signal as a function of time is shown at the leading edge. What is surprising is that the first wave packet and the response in the boundary layer do not intersect on the plate! Thus the receptive response in the boundary layer appears to arise from the second wave packet in the free stream which has a higher phase velocity in the streamwise direction (larger streamwise wavelength) and a correspondingly smaller spanwise wavelength. The response to the leading packet appears to be negligible. This is a surprising result which shows a sensitive difference in receptivity which we subsequently verified with more data. The results at different x locations in Figure 9 show that the leading wave packet in the boundary layer is a direct response to the free stream forcing. Thus we have directly subtracted from the signals in the boundary layer a multiple of the free stream signal immediately above it such that the forced response to the leading packet is practically removed. Figure 16 shows the remaining signals in the boundary layer at two locations after subtraction of the free stream signals and then the remaining signals are shifted to find the wave speed. The result from this shift is a wave speed of 434m/sec. If this subtraction is applied to all the boundary layer signals the resulting x-t diagram is shown in Figure 17. Now it is even clearer that the origin of the instability wave that is growing in the boundary layer (and has a much lower wave speed than the free stream wave packets) is not the first wave packet at the leading edge but the second! This is examined further in Figure 18 in which we show the signals at the leading edge for two wires separated in z by 0.5". The time delay found for each period is used to obtain the spanwise wavelength. The trend is consistent with expectations from figure 6 (b). We see that the spanwise wavelength is relatively large for the first packet (greater than approximately 10 cm) and notably less for the second (2 -8cm). When R is in the range of 500-700, the dimensionless wave numbers of the most unstable waves are in the range of 0.0625 – 0.106 and in table II below we show the spanwise wavelength of instability waves obtained from the stability diagrams provided by Professor Anatoli Tumin (private communication). We see that indeed the spanwise wavelength of unstable waves at the Reynolds number of the experiment is in the range of 1.5 cm to 3.6 cm which is matched much more closely by the second wave packet than the first. This adds considerable support to the hypothesis that it it is a relatively close matching in spanwise wavelength that leads to the receptivity to the second packet and not to the first wave packet.

Up until this point it had not proved possible to drive a u-a free stream disturbance. Through simulation first we then set about a focussed attempt to drive the u-a wave directly from the tunnel sidewall. This was particularly successful and was presented at

the Program Manager's annual program review meeting on August 7th 2007. The presentation is attached.

4. Acknowledgement/Disclaimer

This work was sponsored in part by the Air Force Office of Scientific Research, USAF, under contract number F49620-00-1-0040. The views and conclusions contained herein are those of the authors and should not be interpreted as necessarily representing the official policies or endorsements, either expressed or implied, of the Air Force Office of Scientific Research or the US Government.

5. Personnel Supported

Dr Xuejun Fan, Research Staff Member, Princeton University, Princeton, NJ left the project in approximately May 2004

Dr Zhilei Wu, Research staff member Princeton University, joined the project on August 23 2004

William Stokes, Senior Technician, Princeton University, Princeton, NJ

6. Publications

1. Graziosi, P. and Brown, G. L., Experiments on Stability, Receptivity and Transition for a Compressible Boundary Layer at Mach 3. J. Fluid Mech. 472: 83-124, Dec 10, 2002.
2. Fan, Xuejun and Brown, G.L., Development of Acoustic Forcing for the Studies of Supersonic Boundary Layer Receptivity. Submitted Physics of Fluids
3. Wu, Zheilei and Brown, G.L., Experiments on the receptivity of a compressible laminar boundary layer to free-stream acoustic forcing. In progress

7. Interactions/Transitions

This research has been closely coupled with the research led by Prof. Hermann Fasel at the University of Arizona and with Prof Anatoli Tumin. The experimental work reached a remarkable point where for the first time u+a and u-a acoustic wave-packets were generated and the receptivity of the boundary layer to these very different free stream acoustic wave-packets was measured. No such success in driving acoustic wave-packets in compressible flow and measuring receptivity has ever been achieved prior to this.

8. AFRL Point of Contact

Dr. Roger Kimmel Tel 937 255 6813. Contact has been by telephone and email.

9. References

1. Graziosi, P. and Brown, G. L., 2002 "Experiments on Stability, Receptivity and Transition for a Compressible Boundary Layer at Mach 3," J. Fluid Mech. 472: 83-124.

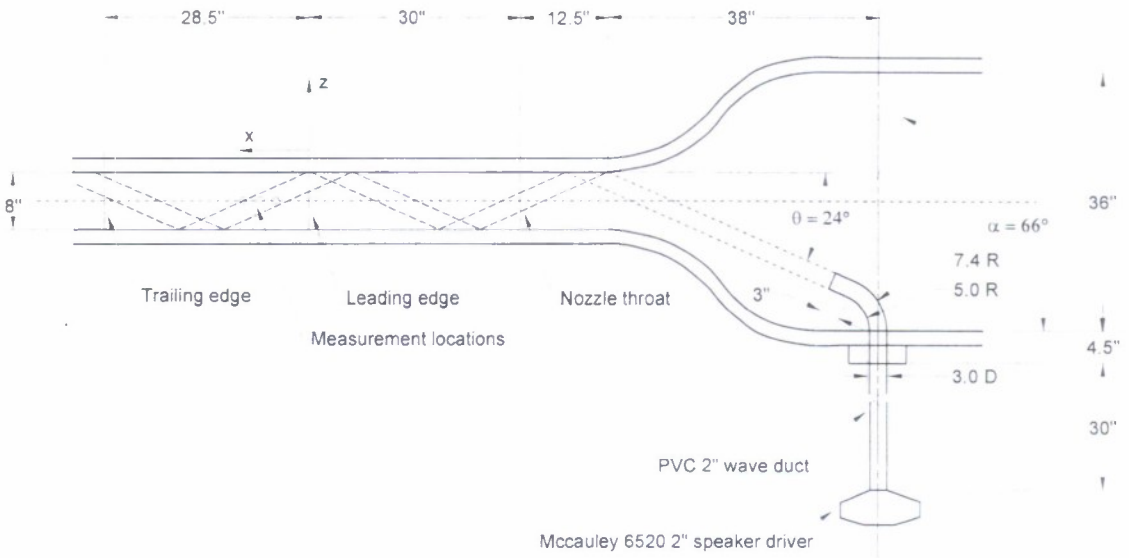

Figure 1. Speaker driver with 66^0 wave duct.

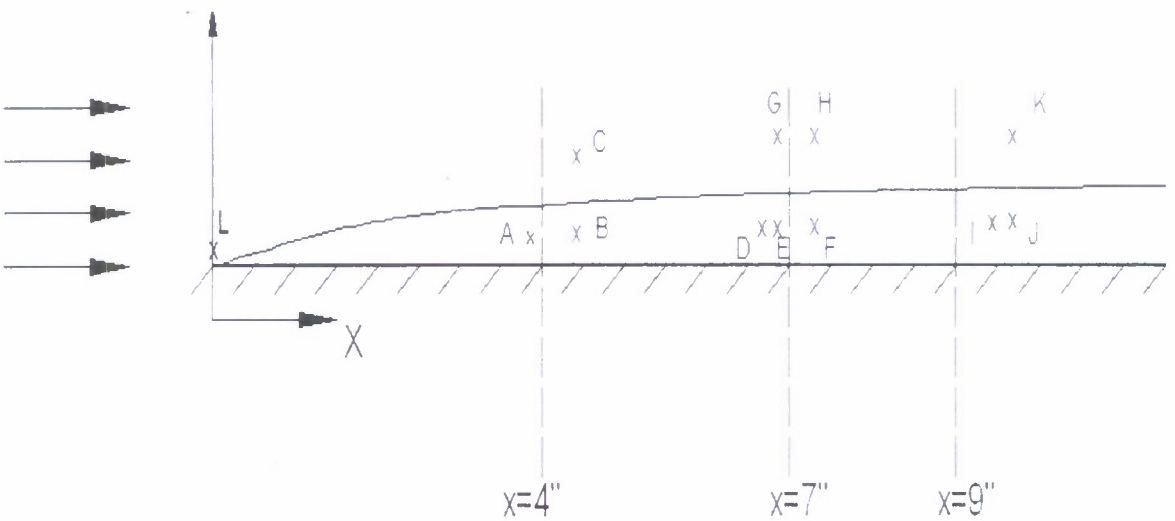

Figure 2. The locations of the hotwires at which the data for this report has been taken

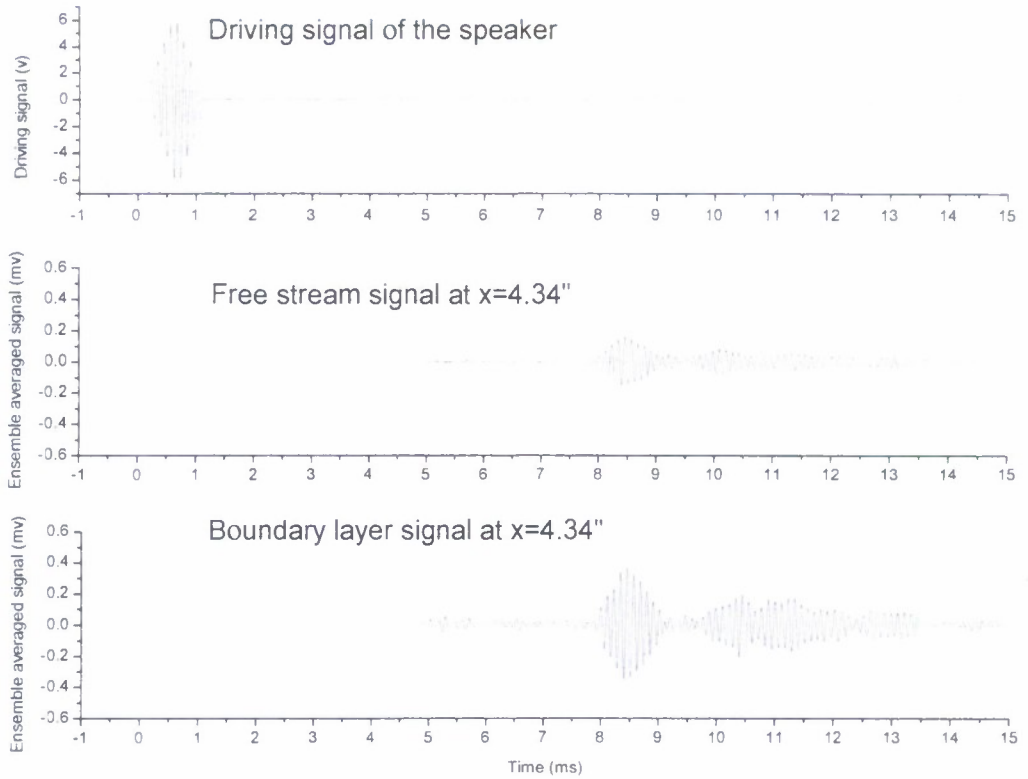

Figure 3. Driving voltage and wave packet in the free stream: f = 8.9khz, 8 waves.

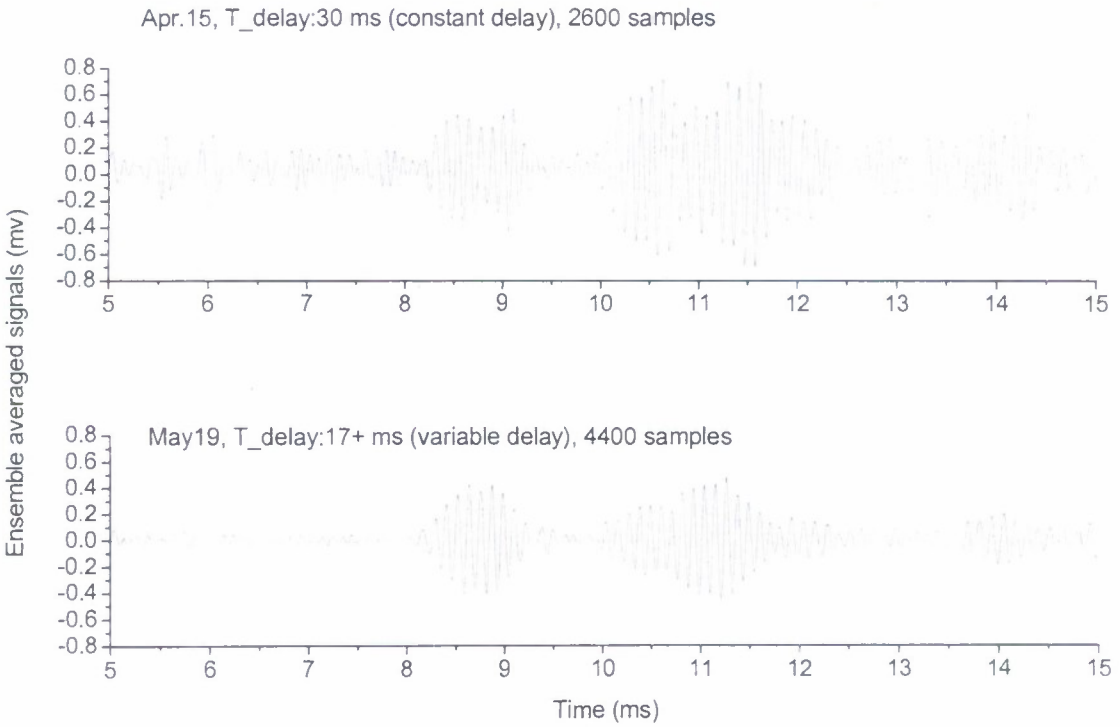

Figure 4. Comparison of noise rejection for signals in the boundary layer at x=9.31", y/(x/R)=7.1

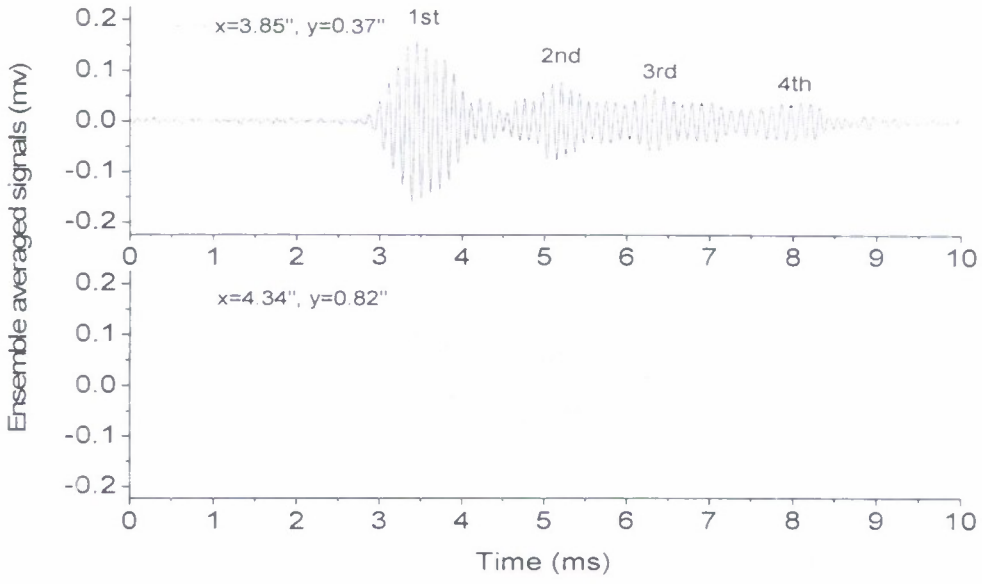

(a)

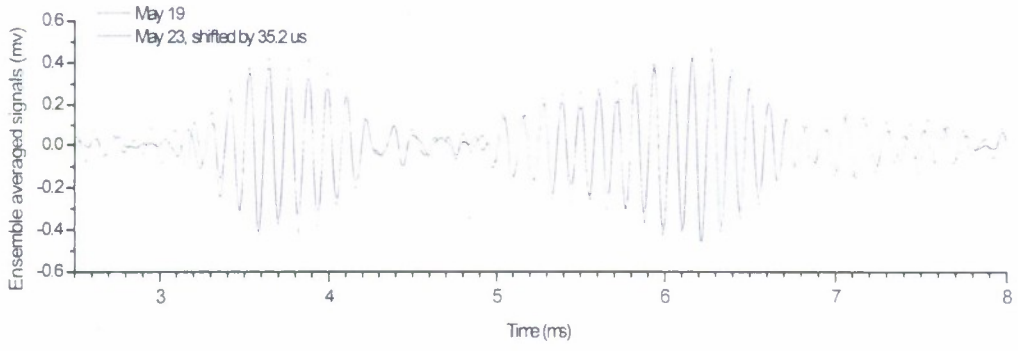

(b)

Figure 5. (a)Simultaneous measurements in the free stream at two x locations
(b) Signals measured in the boundary layer at the same location :x =9.31", y/(x/R)=7.1 but on different days.

	Rms Raw data* (uv)	Rms After ensemble average (uv)	Ratio Raw/Ens emble A.
Free stream	872	12.6	69.2
Boundary layer	2533	47.9	52.9

(a)

	Rms Raw data (uv)	Rms After ensemble average (uv)	Ratio Raw/Ens emble A.
Free stream	255	3.4	75.4
Boundary layer	1275	19.6	65.1

(b)

Table 1. Noise rejection
(a) Data from x_f=x_b=9.59";(b) Data from x_f=x_b=4.34"
Raw data: refers to the signals that have already been band-pass filtered (8KHZ-10KHZ)

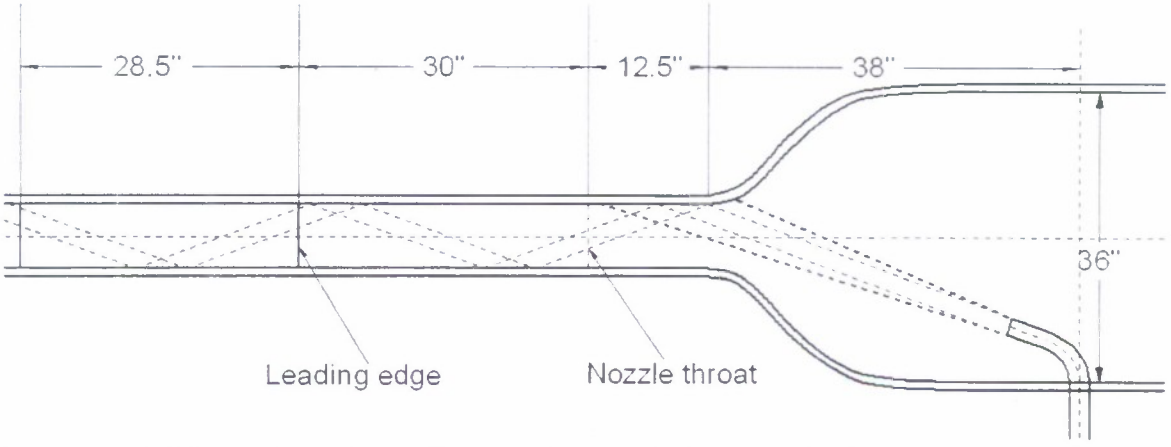

Figure 6 (a). The propagation of the sound waves in the tunnel, without a spreading angle

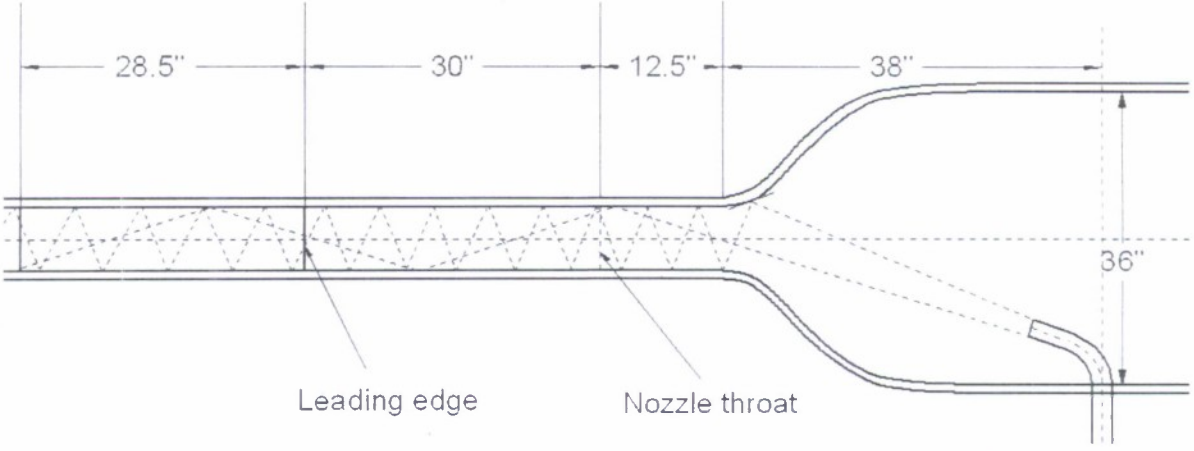

Figure 6 (b). The propagation of the sound waves in the tunnel, with a spreading angle

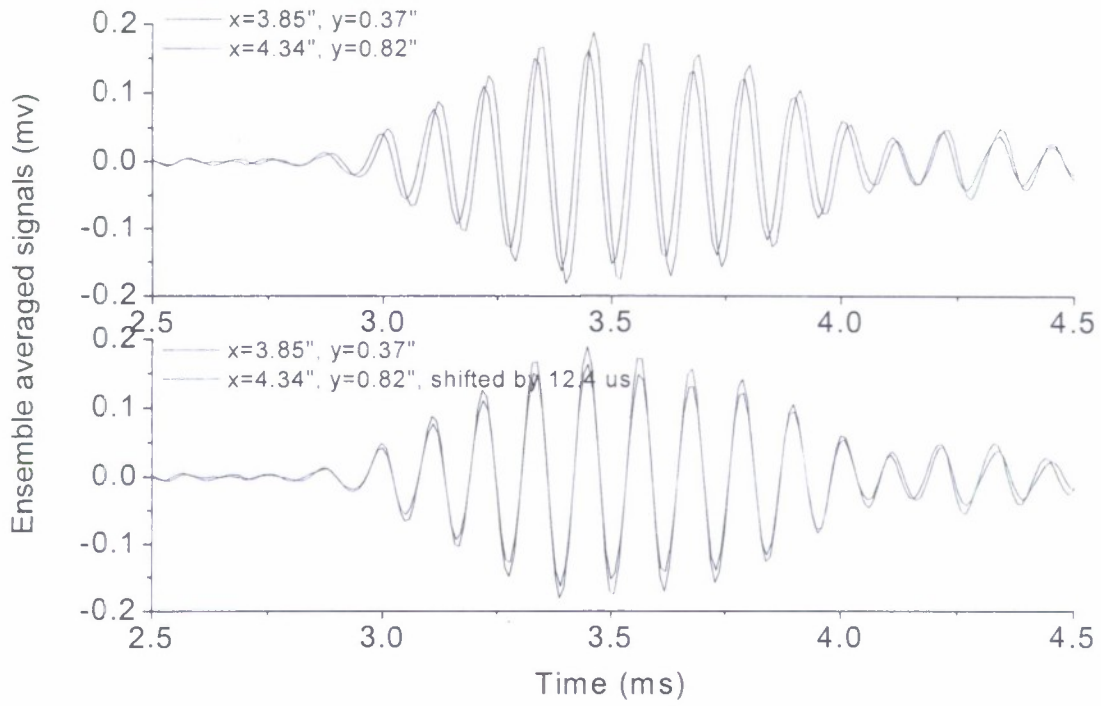

Figure 7. Simultaneous Measurements in the free stream at two locations and then one shifted in time to align the first packet.

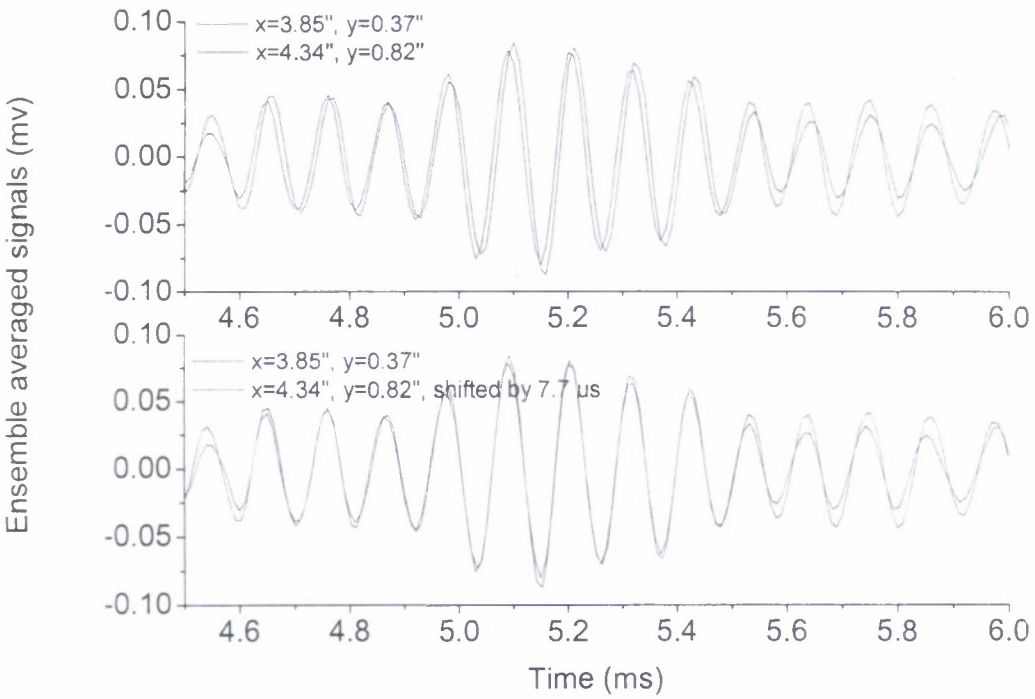

Figure 8. Simultaneous Measurements in the free stream at two locations and then one shifted in time to align the second packet. (Note the shorter time delay compared with the first packet result in Figure 7 (7.7 compared with 12.4 micro seconds))

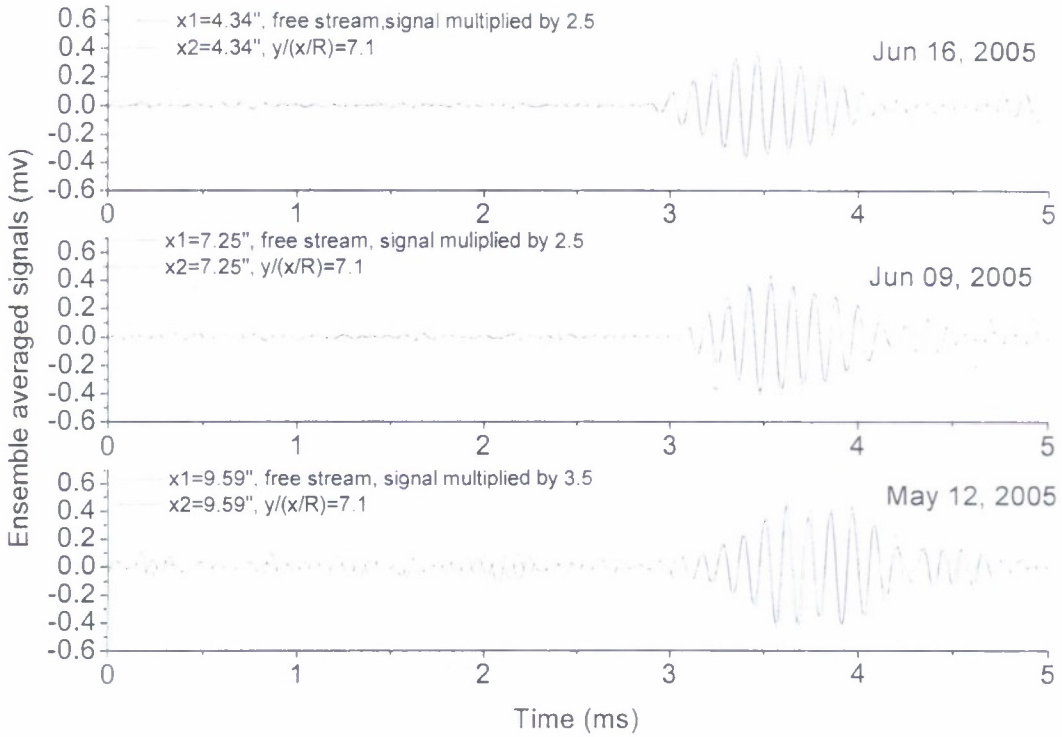

Figure 9 First wave packet in the free stream and the forced response to it in the boundary layer at three x locations

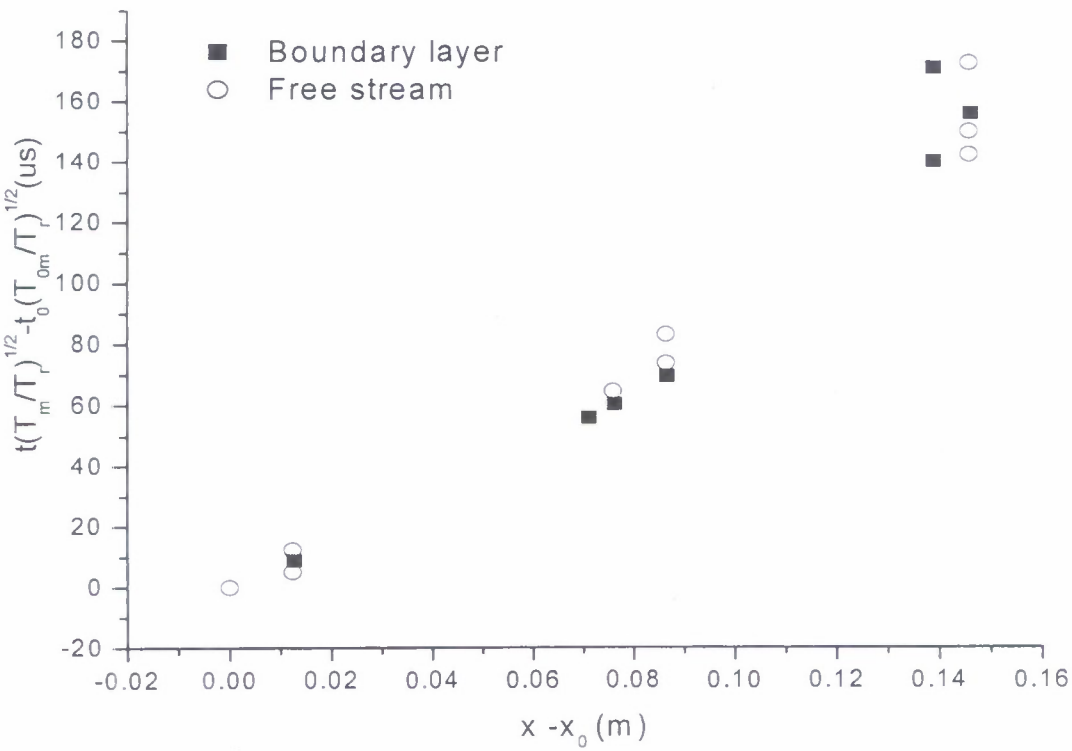

Figure 10. x-t diagram where the measured arrival time is rescaled using the measured temperature and a reference temperature of T_r=297.65 °C.

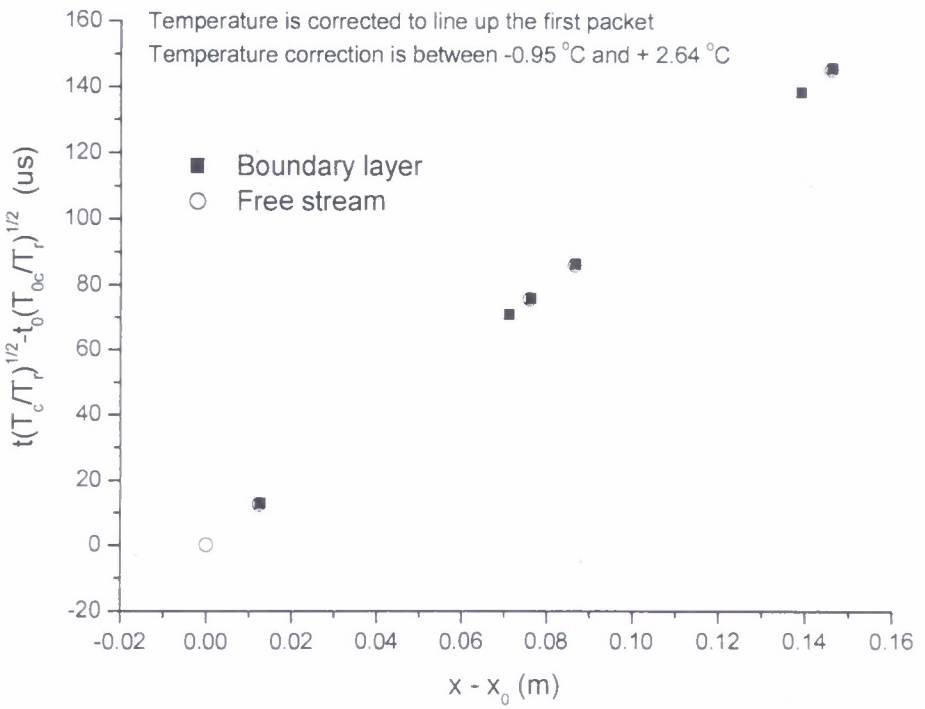

Figure 11. x-t diagram. The measured temperature has been corrected to give a constant phase speed, at a reference temperature, for the first wave-packet in the free stream and the boundary layer.

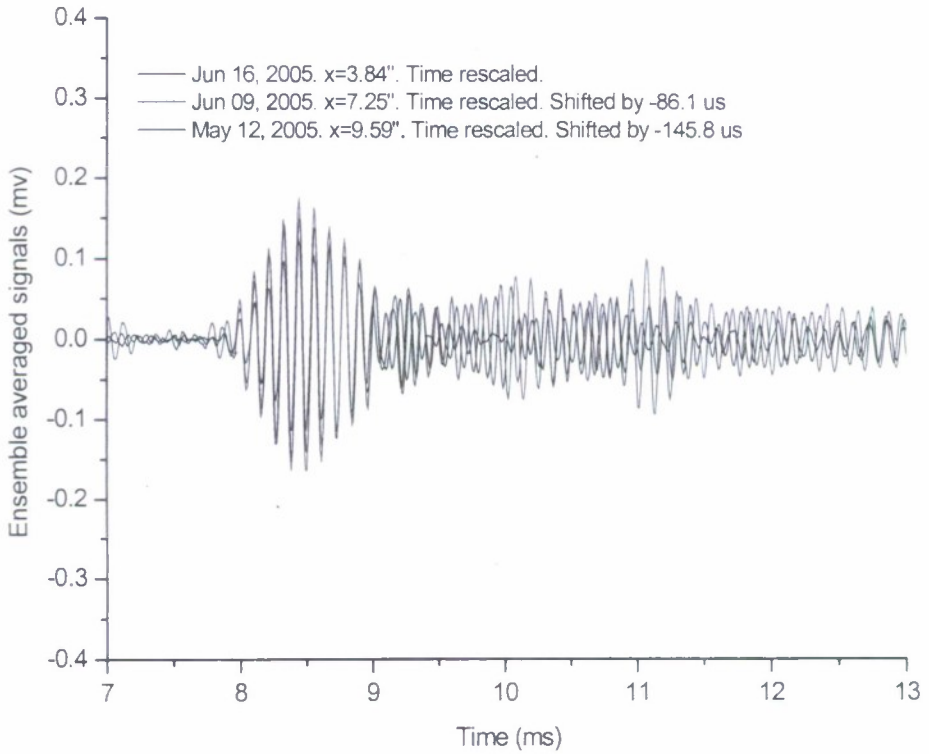

Figure 12. Signals in the free stream from different x locations. Arrival time is rescaled as in figure 11. The signals are shifted to align the first wave packet

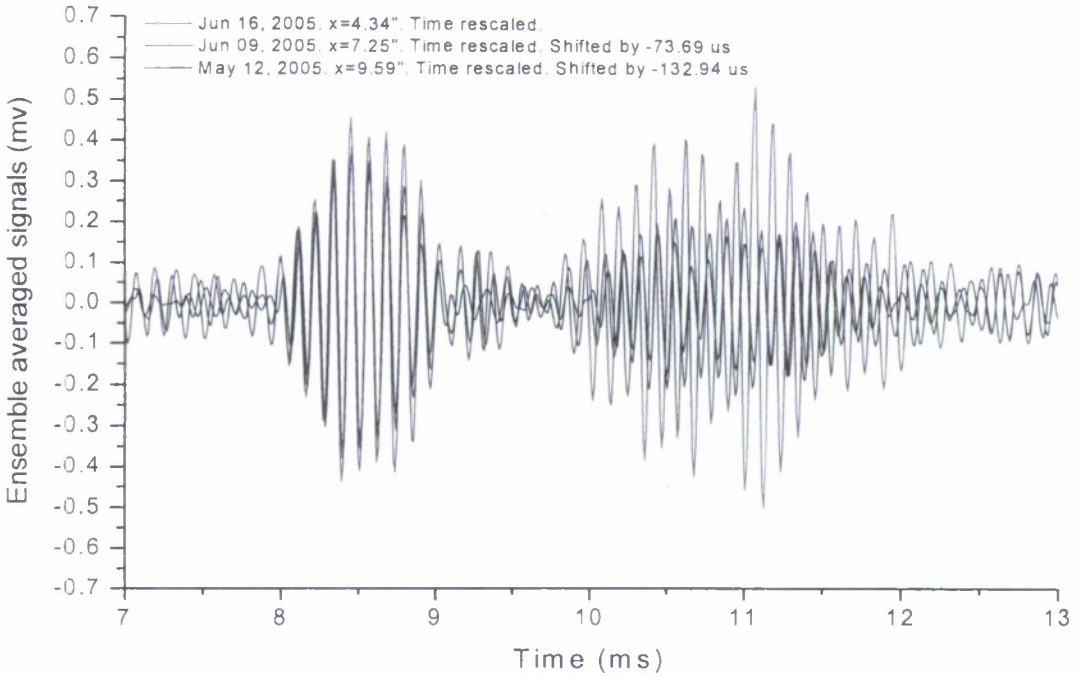

Figure 13. Signals in the boundary layer (y/(x/R)=7.1) from different x locations. Arrival time is rescaled as in figure 11. The signals are shifted to align the first wave packet

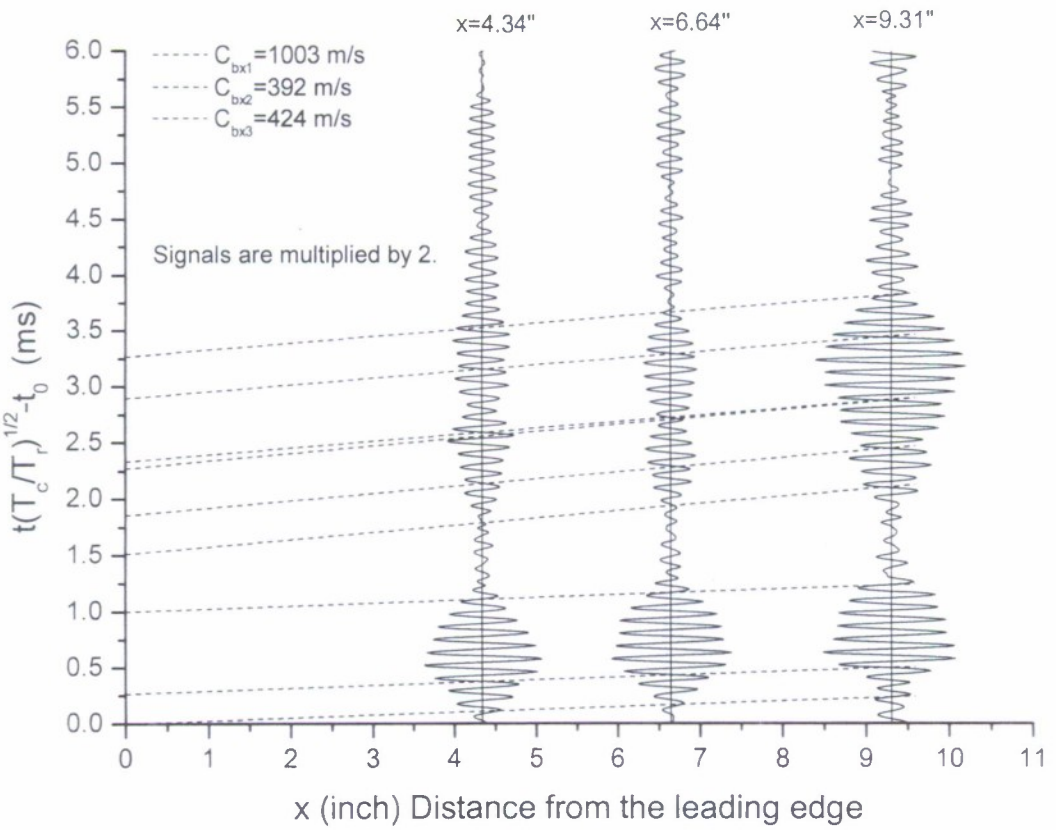

Figure 14. x-t Diagram for signals in the boundary layer

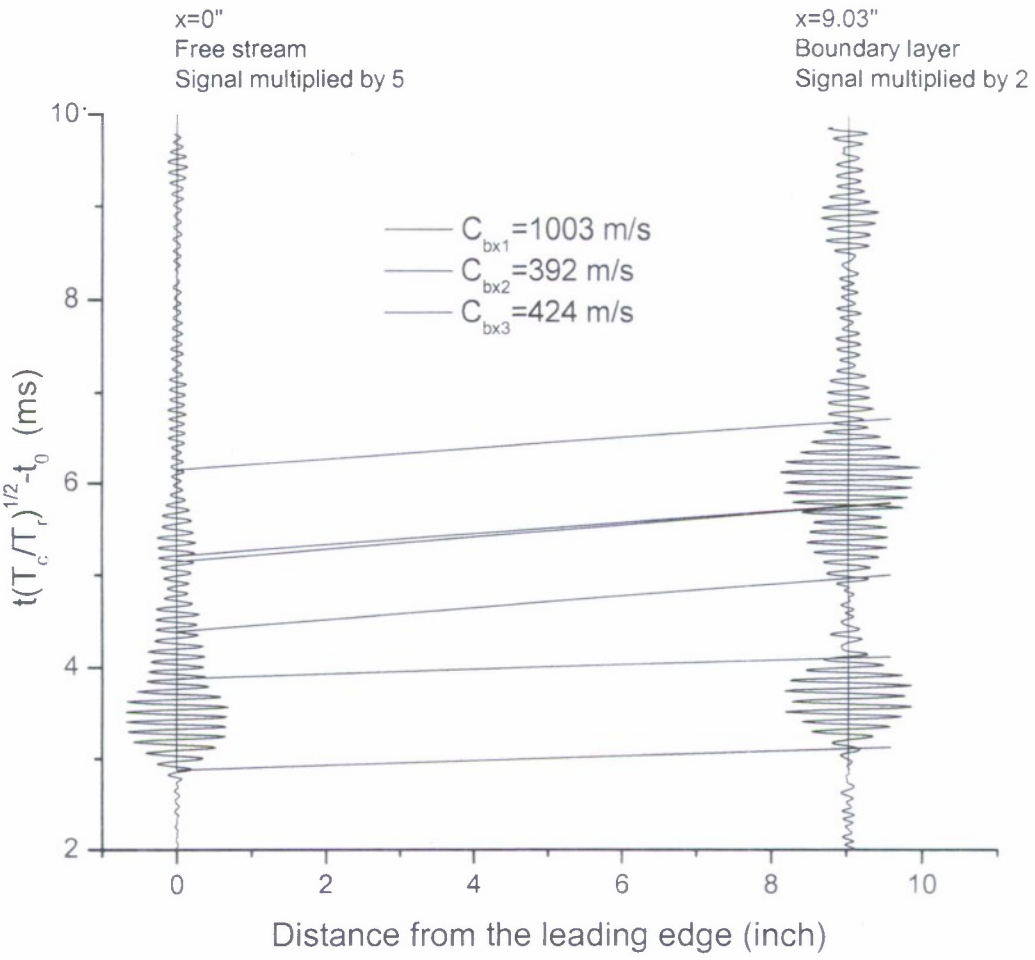

Figure 15. x-t Diagram for signals in the freestream at the leading edge and downstream in the boundary layer at 9.03"

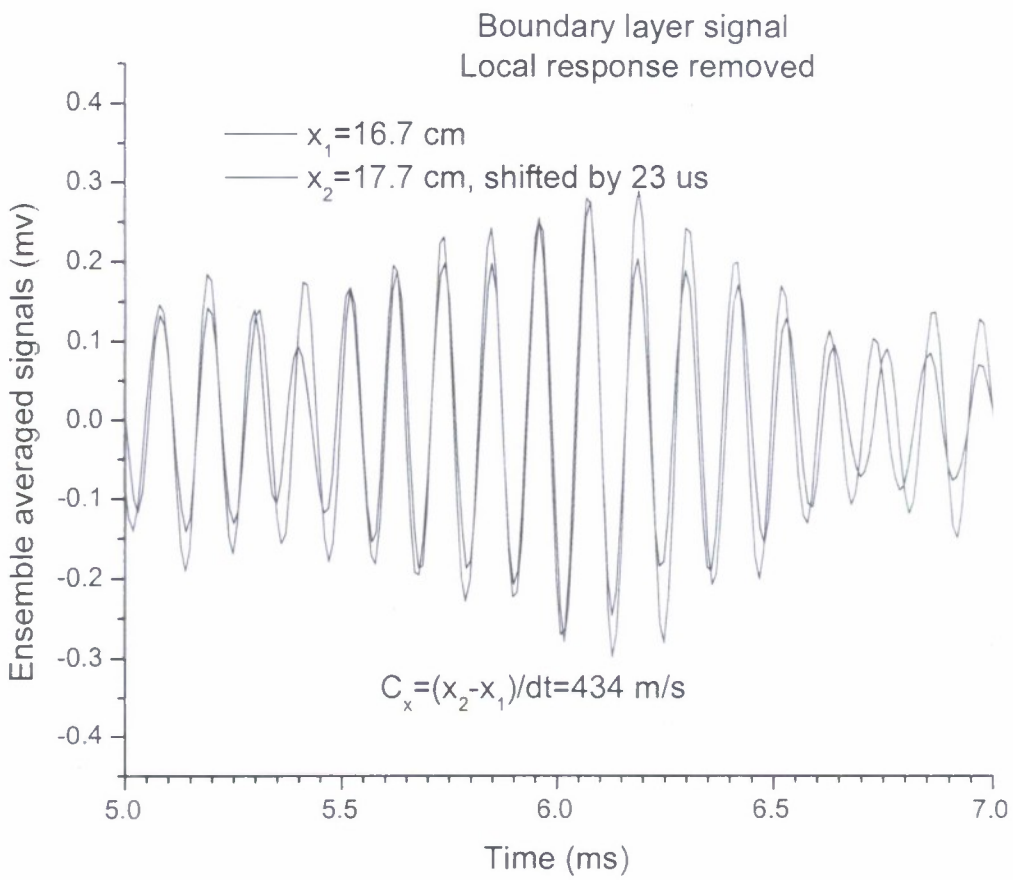

Figure 16. Signals in the boundary layer at two locations after subtraction of the the free stream signals such that the forced response to the leading packet is practically removed and the remaining signals shifted to find the wave speed.

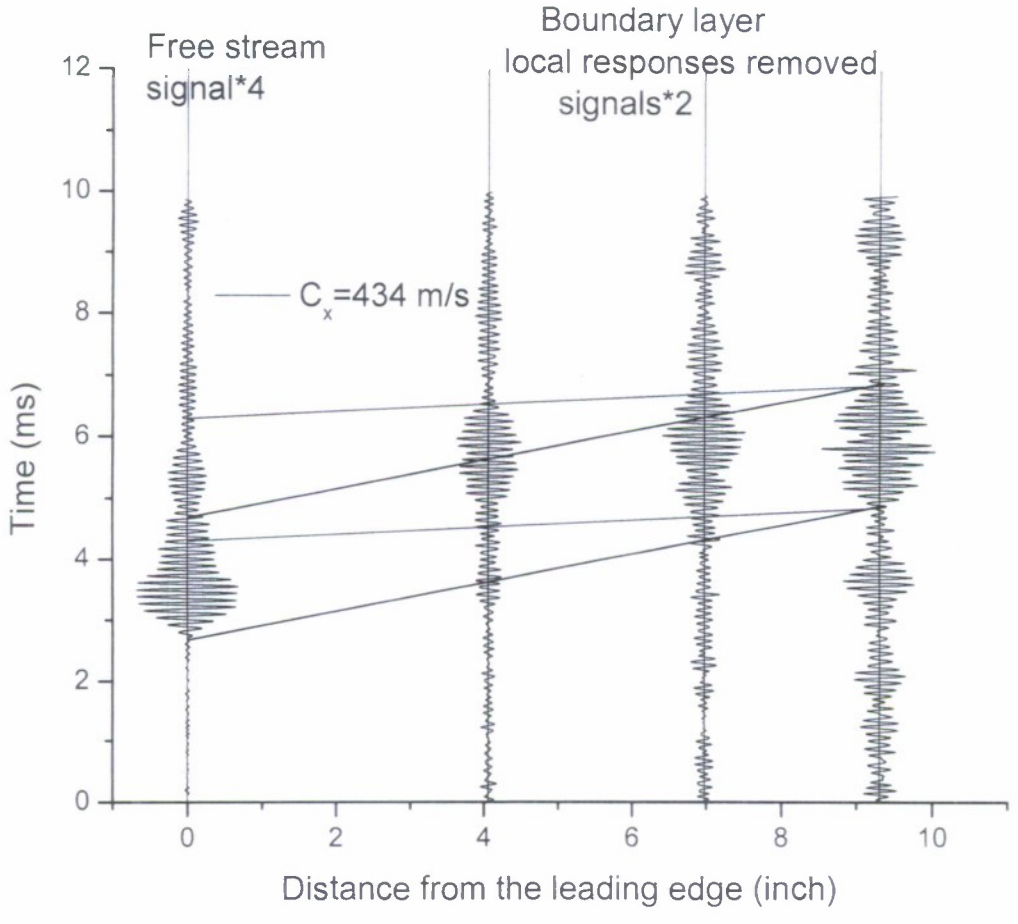

Figure 17. x-t Diagram of the signal in the free stream at the leading edge and downstream in the boundary layer at three locations **after** subtraction of the free stream signals such that the forced response to the leading packet in the boundary layer (evident in Figure 14) is practically removed.

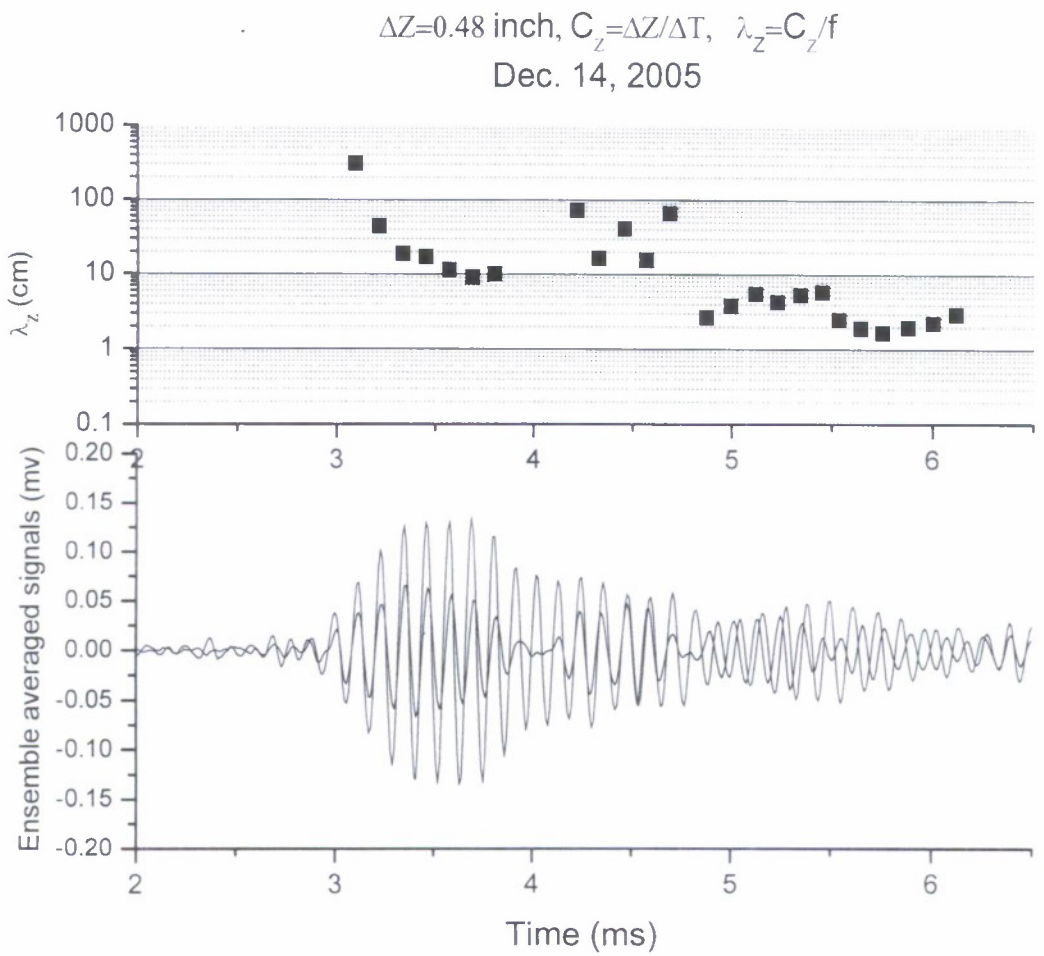

Figure 18 Calculated spanwise wavelength obtained from the signals from two wires at the leading edge, separated by 0.5" The wavelength is found from the time delay for each period

λ_z(cm) R / β*	500 (x=5.07")	550 (x=6.12")	600 (x=7.30")	650 (x=8.54")	700 (x=9.93")
0.0625	2.58	2.83	3.09	3.34	3.60
0.084	1.93	2.11	2.31	2.49	2.69
0.106	1.52	1.67	1.82	1.97	2.12

Table II : λ_z (wave length in Z direction) of the most unstable waves

(When R is in the range of 500-700, the dimensionless wave numbers of the most unstable waves are in the range of 0.0625 – 0.106